International Journal of High Energy Physics
2026, Vol. 12, No. 1, pp. 9–19
https://doi.org/10.11648/j.ijhep.20261201.12

SciencePG
Science Publishing Group

Research Article

Investigation of Solar Eclipse-induced Variations in Total Electron Content over Ethiopia During 26 January 2009 and 20 March 2015

Debrie Ayalew[1, *], Shambel Gizachew[2], Melkamu Habtamu[3]

[1]Department of Physics, Debre Markos University, Debremarkos, Ethiopia
[2]Department of Physics, College of Natural and Computational Science, Debremarkos, Ethiopia
[3]Werbecha Secondary School, Hossana, Ethiopia

Abstract

Solar eclipses provide unique opportunities to study how the ionosphere responds to rapid changes in the ionization rate. The partial solar eclipse of January 26, 2009, and the partial solar eclipse of March 20, 2015, offered opportunities to understand ionospheric electron density variations along the annularity path during solar minimum and geomagnetic quiet periods. For this analysis, various ground-based GPS stations located along the annularity line were selected and divided into three major regions: namely, Bahir Dar, Arbaminch, and Robe stations. We analyzed the temporal and spatial vertical total electron content (VTEC) variations before, during, and after these events, while comparing the observed changes between the two eclipse periods. On January 26, the eclipse day, a noticeable depression in VTEC is observed during the eclipse interval, which began at 04: 57 UT, reached its maximum obscuration (55 - 65% coverage) at 07: 59: 44 UT, and ended around 09: 55 UT. This reduction corresponds to the temporary decrease in solar radiation reaching the Earth's ionosphere. The VTEC variations observed over the Bahir Dar station during January 25-27, 2009, clearly demonstrate the ionospheric response. On the non-eclipse days (January 25 and 27, 2009), the TEC followed a normal diurnal trend, increasing after sunrise, peaking around midday, and decreasing toward night. In contrast, on the eclipse day, the TEC curve shows a pronounced depression during the eclipse interval. The comparison of TEC variation on consecutive days reveals that, on the reference day of 19 March 2015 (before the eclipse), the maximum VTEC was approximately 26 TECU. In contrast, on 20 March 2015 (the eclipse day), the maximum VTEC was approximately 24 TECU. This clearly demonstrates the effect of the partial solar eclipse on March 20, 2015, over BDR. The VTEC variations observed at the BDR station on 20 March 2015 show an approximate 20% reduction, corresponding to the temporary decrease in solar radiation reaching Earth's ionosphere.

Keywords

Solar Eclipse, VTEC, Geomagnetic Storm, Ionospheric Variability

*Correspondence: Debrie Ayalew (debrieayalew@gmail.com)

Received: 25 March 2026; **Accepted:** 7 May 2026; **Published:** 26 May 2026

1. Introduction

The ionosphere is the ionized region of upper atmosphere that varies from place to place and from time to time [1, 2]. It affects the propagation of radio waves, so to examine ionospheric variation is crucial for navigation and telecommunication [1, 3].

The ionosphere is primarily created through the photoionization of neutral molecules caused by solar extreme ultraviolet (EUV) and soft X ray radiation in the sunlit hemisphere [4, 5]. However, variations in its composition and behaviour also depend on changes in EUV intensity, as well as levels of solar and geomagnetic activity [6, 7].

The ionosphere, an ionized layer in Earth's upper atmosphere, contains enough free electrons to significantly impact radio wave propagation. As a dispersive medium, it profoundly affects satellite navigation and communication systems [8, 9].

Theoretically, different periods of ionospheric physical process can be studied by detecting and analyzing the temporal variations of TEC [10, 11]. TEC is characterized by spatial and temporal variations that can be traced primarily to changes in solar radiation with time and geographic location, magnetic activity and solar eclipse [12].

During a solar eclipse, the Earth's ionosphere experiences significant effects, including total electron content (TEC), plasma frequency, and radio propagation [13].

A solar eclipse is an event that directly impacts the Earth's ionosphere. This phenomenon causes noticeable changes in the ionosphere [14]. It happens when the Moon moves between the Earth and the Sun, putting its shadow on the Earth and completely or partially blocking the Sun from the perspective of an observer on Earth [13, 15].

Eclipses are connected with the rapid and short time, impulse-like decrease of the solar energy flux reaching the area of its visibility, which can be exactly predicted before the occurrence of the phenomenon [15, 16].

Solar eclipses offer a unique opportunity to examine how rapid decreases and increases in solar radiation over a short time period impact various regions of the Earth's atmosphere. Consequently, numerous previous studies have investigated the response of the upper atmosphere and ionosphere to solar eclipses [15, 17]. During a solar eclipse, the Sun's radiation that reaches Earth decreases, leading to reduced ionization of atoms and a lower electron density in the ionosphere [18].

A solar eclipse is a natural phenomenon that occurs when the moon appears between the Sun and the Earth, and the moon fully or partially blocks the Sun, casting a shadow over the Earth [19]. When a solar eclipse occurs, with the Moon positioned between the Sun and the Earth, it can lead to changes in the ionosphere [20]. The reduction in solar radiation causes a decrease in ultraviolet (UV) solar flux, which in turn impacts all ionospheric layers [19]. A total solar eclipse causes an abrupt and brief drop in solar radiation, which can lead to a significant decrease in the ionospheric electron density (Ne) around the time of maximum coverage [21, 22]. This decrease in TEC during the eclipse period can have significant effects on radio wave propagation and communication systems [23]. Several studies have previously investigated how solar eclipses affect the ionospheric total electron content (TEC) at various locations around the Earth [21].

This study seeks to determine the key parameters of ionospheric total electron content variations caused by the partial solar eclipses on January 26, 2009, and March 20, 2015, using GPS data gathered from three Ethiopian stations.

2. Study Area Description, Data Source and Methodology

2.1. Study Area Description and Data Sources

We analyzed the response of ionospheric TEC variation during partial solar eclipse events, GPS (Global Positioning System) dual-frequency observation data were collected from three Ethiopian stations: Bahir Dar (11.6°N, 37.4°E), Arbaminch (6.0°N, 37.6°E), and Robe (7.1°N, 40.0°E). These data were used to observe ionospheric TEC variations during the solar eclipses on 26 January 2009 and 20 March, 2015 occurred during different solar Cycle.

The ionospheric TEC data were obtained from the UNAVCO (University NAVSTAR Consortium) website. Data gained from this web, used to estimate the TEC along a ray path between a GPS satellite and receiver on the ground [24]. The experimental VEC finally import in to MATLAB work space and analyze the data. Additionally, geomagnetic indices Kp and Dst data for the studied events were retrieved from astronomical data. This study seeks to examine solar eclipse-induced TEC variations across Ethiopia by assessing temporal and spatial changes during the partial solar eclipses of January 26, 2009, and March 20, 2015, while comparing the responses from stations at Bahir Dar, Robe, and Arbaminch.

2.2. Methodology

Total electron content (TEC) serves as a key parameter for characterizing Earth's ionosphere. It quantifies the total number of electrons along a GPS signal's path from satellite to receiver through the ionosphere. TEC is expressed in TECU, where $1TECU = 1x\ \ 10^{16}e/\ m^2$ [24, 25]. From a physical standpoint, the total electron content is, to first order, defined as the line integral of the electron density along the signal path between the GPS satellite and the ground receiver [26-28].

The wave propagation through the medium is characterized by index of refraction, and can be expressed as follows:

$$n = \frac{c}{v} \tag{1}$$

Whre c is the speed of light in vacuum, and v, is the velocity of the wave in medium.

The ionosphere is not a homogenous medium. The phase index of refraction at a given location in the ionosphere, n_p, can be expressed by the Appleton-Hartree formula.

$$n_p^2 = 1 - \frac{X}{1 - jZ - \frac{yT^2}{2(1-X-jZ)} \pm \sqrt{\frac{yT^4}{4(1-X-jZ)^2} + YL^2}} \quad (2)$$

Where $X = \frac{N_e e^2}{\varepsilon_0 m\omega^2} = \frac{\omega_p{}^2}{\omega^2}$

$$Y_L = \frac{eB_L}{m\omega} = \frac{\omega_{Hcos\theta}}{\omega}$$

$$Y_T = \frac{eB_T}{m\omega} = \frac{\omega_{Hsin\theta}}{\omega}$$

$$Z = \frac{v}{\omega}, \omega = 2\pi f$$

Where f is the system operating frequency in Hz, in our case the GPS frequency.

e = electron charge (e = −1.602 × 10^{-19} C)

ε is permittivity of free space (ε = 8.854×10^{-12} Fm^{-1})

m = rest mass of an electron

(kg =9.107 × 10^{-31})

θ= the angle of the ray with respect to the Earth's magnetic field.

v the electron-neutral collision frequency

ω_H the electron gyro frequency.

N_e the electron density, and the L and T subscripts refer to the transverse and longitudinal components of the magnetic field. The plus and minus sign in equation (2) indicates that the complex refractive index may take two different values.

For an electromagnetic wave at ultra-high frequencies (UHF), as is the case for GPS signals, both the electron-neutral collisions and the effects of the geomagnetic field on the refractive index are negligible ($Y_T = Y_L = Z = 0$). In such case the refractive index has only a real part.

$$n_p^2 = 1 - X = 1 - \frac{\omega_p{}^2}{\omega^2} \quad (3)$$

At UHF X <<1 and so the Binomial theorem can be used to then obtain:

$$n_p = 1 - \frac{X}{2} = 1 - \frac{N_e e^2}{2\varepsilon_0 m\omega^2} = 1 - \frac{N_e e^2}{8\pi^2 \varepsilon_0 m f^2} = 1 - \frac{KN_e}{2f^2} \quad (4)$$

Where $K = \frac{e^2}{4\pi^2 \varepsilon_0 m} = 80.69 \ \ {}^{m^3}/_{S}$.

By substituting values of constants e, m and ε_0 in equation (3), the phase index of refraction can be expressed by

$$n_p = 1 - \frac{40.3N}{f^2} \quad (5)$$

Therefore, the phase index of refraction mainly depends on the electron density N, and the radio-wave frequency.

The group index of refraction can be derived from the relation:

$$n_g = n_p + \frac{f d_{np}}{df} = \left(1 - \frac{40.3N}{f^2}\right) + \frac{80.3fN}{f^3} = 1 + \frac{80.3N}{f^2} \quad (6)$$

The group delay can be written as:

$$I_{\emptyset,g} = \frac{80.6}{2f^2} \int n_e ds = \frac{40.3}{f^2} TEC(m) \quad (7)$$

All GPS satellites transmit on two L band frequencies (f_1=1575.42MHz) and (f_2=1227.60MHz), both derived from a base frequency (f_0=10.23MHz). By measuring the ionospheric group delay and carrier phase advance on the L_1 and L_2 signals, the STEC (slant TEC) the TEC along the line-of sight path can be computed as follows [24, 29]:

$$STEC = \int_R^S n_e ds \quad (8)$$

Where STEC total electron content $[m^{-2}]$.

During data processing, we apply a single shell ionosphere model at an altitude of 400 km Where S and R stands for satellite and receiver respectively. n_e is the ionosphere electron density [30]. In calculating the TEC the ionosphere is considered as a thin shell and the ionosphere pierce point (IPP), which is the point at which the signal from the satellite just inters ionosphere, is at 400 km from the Earth's surface.

$$I_{\emptyset,g} = \frac{80.6}{2f^2} \int n_e ds = \frac{40.3}{f^2} TEC(m) \quad (9)$$

Where$I_{\emptyset,g}$ represents the group and phase delay. A dual frequency GPS receiver measures the ionospheric delay between the f_1 and f_2 signals [26, 31].

This can be written as

$$P_2 - P_1 = 40.3TEC\left(\frac{1}{f_2^2} - \frac{1}{f_1^2}\right) \quad (10)$$

Where P_2 and P_1 are the group lengths of f_1 and f_2. f_1 and f_2 are the corresponding frequencies. Rearranging this we get TEC as

$$TEC = \frac{1}{40.3}\left[\frac{f_1^2 f_2^2}{f_2^2 - f_1^2}\right](P_2 - P_1) \quad (11)$$

STEC can be converted to vertical TEC (VTEC) by assuming the penetration point of the satellite signal with the ionosphere thin shell at a height of 400 km (f_2 region peak) [32].

$$VTEC = cos\mathcal{X}.(STEC) \quad (12)$$

Where $\mathcal{X}$ is the angle of incidence at 400 km of the GPS ray path from satellite to ground receiver. An oblique factor $cos\mathcal{X}$ is defined as

$$cos\mathcal{X} = \sqrt{1 - \left(\frac{R_E cose}{R_E + h_m}\right)^2} \quad (13)$$

According to STEC conversion to VTEC has deficiencies. This is because electron density is assumed to be concentrated in a two dimensional layer at a height of 400km [33, 34].

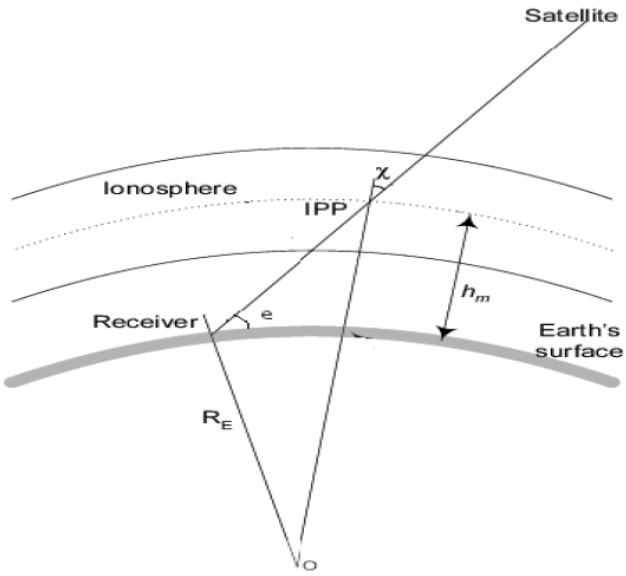

Figure 1. *To determine its total electron content, the ionosphere is modeled as a thin shell at a nominal height of 400 kilometers [34].*

3. Results and Discussion

The impact of solar eclipses on the ionosphere TEC is significant due to the sudden reduction in solar radiation, which temporarily disrupts ionization processes in the ionosphere. The magnitude of TEC reduction depends on factors such as eclipse magnitude, local time, season, and geographic location. Such variations provide valuable opportunities to study the dynamic behavior of the ionosphere under abrupt solar forcing conditions [13].

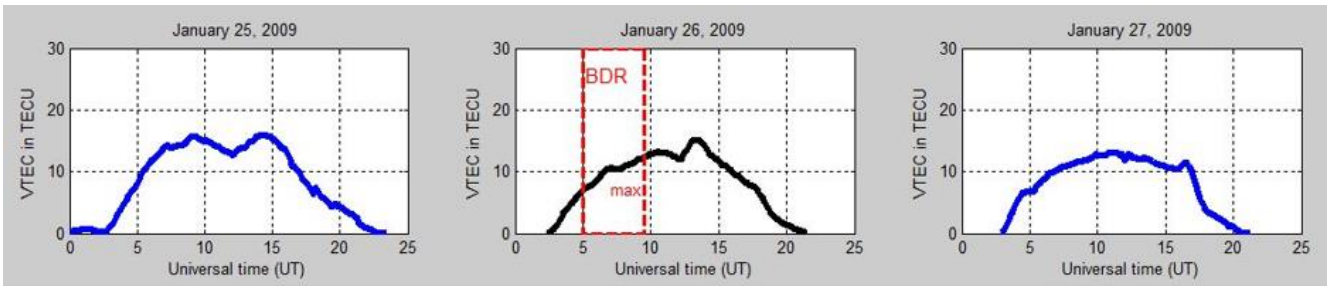

Figure 2. *The variations in VTEC at the BahirDar station during the days before, during, and after the partial solar eclipse on January 26, 2009.*

The above three graphs present the VTEC variation over BahirDar station during the days surrounding the partial solar eclipse of January 26, 2009. On the reference days, January 25 and 27, the VTEC values show a typical diurnal pattern, gradually increasing after sunrise, peaking during midday, and then decreasing toward nighttime. However, on January 26, the eclipse day, a noticeable depression in VTEC is observed during the eclipse interval, which began at 04: 57 UT, reached its maximum obscuration (55 - 65% coverage). On the reference day, 25 January 2009, before the eclipse, TEC varies during the eclipse period (5 UT to 09: 57 UT) from 10 TECU to 18 TECU. After the eclipse day, on 27 January 2009, TEC varies from 10 TECU to 14 TECU. However, on the eclipse day, 26 January 2009, TEC varies from 7 TECU to 12 TECU, which is the minimum compared to the selected reference days.

This reduction corresponds to the temporary decrease in solar radiation reaching the Earth's ionosphere. Limiting ionization and thus lowering the electron density compared to non-eclipse days. After the eclipse ended, the VTEC trend gradually recovered and followed a relatively normal pattern. This clearly illustrates the ionospheric response to the solar eclipse, where reduced solar EUV flux during the obscuration period directly suppressed the ionization process [35, 36]. The VTEC variations observed over the Bahir Dar station during January 25-27, 2009, clearly demonstrate the ionospheric response to the partial solar eclipse of January 26, 2009. On the non-eclipse days (January 25 and 27, 2009), the TEC followed a normal diurnal trend, increasing after sunrise, peaking around midday, and decreasing toward night. This reduction resulted from the temporary suppression of solar EUV radiation, which limited photoionization and reduced electron density in the ionosphere. Although the TEC gradually recovered after the eclipse ended, its peak remained lower than on the reference days. This behavior highlights the sensitivity of the ionosphere to sudden changes in solar radiation and confirms the direct impact of the eclipse on ionospheric electron content.

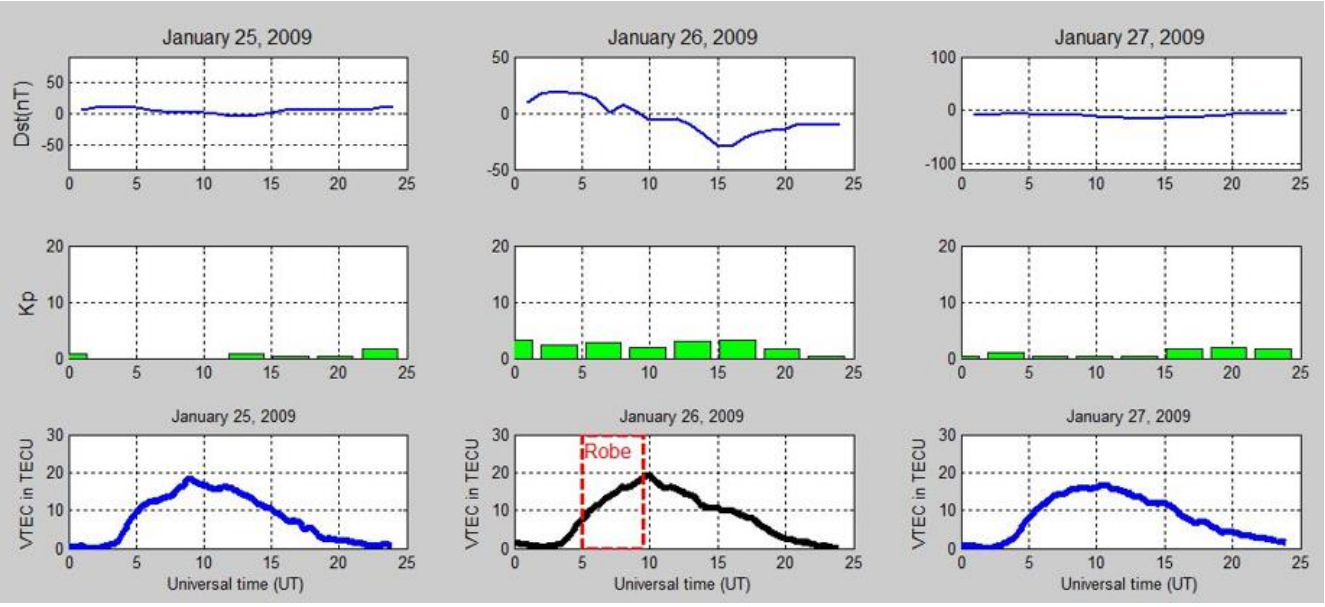

Figure 3. *This shows the diurnal variations of the vertical total electron content (VTEC) and geomagnetic disturbance (with Dst and Kp indices) at Robe station during the days surrounding the partial solar eclipse of January 26, 2009.*

The graph provides a detailed view of the ionospheric effects Robe station from 04: 57 UT to 09: 55 UT, with maximum coverage of 50 - 60%. On the reference day of 25 January 2009, before the eclipse, TEC varied from 11 TECU to 19 TECU during the eclipse period (05: 00–09: 57 UT). On 27 January 2009, TEC ranged from 10 TECU to 17 TECU. On the eclipse day of 26 January 2009, TEC varied from 9 TECU to 18 TECU. Thus, TEC was not at its minimum on the eclipse day compared to the reference days (25 and 27 January 2009), as the eclipse day was more geomagnetically disturbed. On this eclipse day, TEC values were also affected by other factors, such as a geomagnetic storm.

When comparing the three consecutive days January 25 (pre-eclipse), January 26 (eclipse day), and January 27 (post-eclipse) of 2009 distinct variations in VTEC behaviour are observed over Robe station. On the non-eclipse days (January 25 and 27), the VTEC shows a typical diurnal pattern, increasing gradually after sunrise and reaching a maximum value of about 15 - 18 TECU around local noon, mainly due to strong solar radiation and enhanced ionization. In contrast, on the eclipse day (January 26), which featured a partial solar eclipse, the VTEC curve shows a noticeable depression between about 04: 57 UT and 09: 55 UT (the red-dotted interval), corresponding to the time of maximum obscuration. The maximum TEC on this day is lower, reaching only around 18 TECU, indicating that the partial eclipse reduced the available solar radiation and thus the ionization rate in the ionosphere [37].

The rate of increase of TEC before the eclipse maximum was slower compared to the normal days because sunlight was gradually blocked, reducing photoionization. After the eclipse ended, the TEC began to recover but with a slower rise. Meanwhile, both $(D_{st} \approx -30nT)$ and $(K_p < 4)$ values indicate quiet to slightly disturbed geomagnetic conditions, confirming that the observed variations were mainly due to the eclipse rather than geomagnetic activity [38, 39].

Overall, the comparison clearly shows that the partial solar eclipse produced a weaker but observable reduction in TEC, with a lower peak value and slower increase rate than on the other quiet days consistent with the reduced solar energy input during partial obscuration.

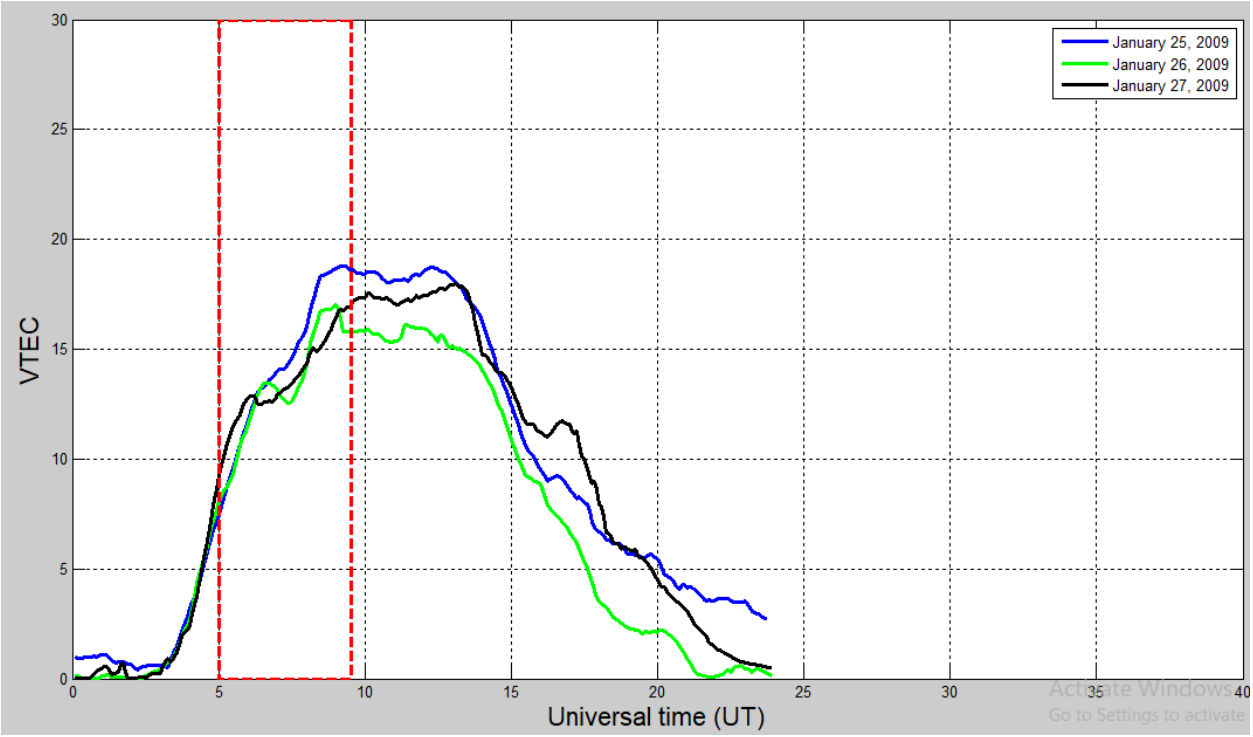

Figure 4. *Shows the diurnal variations of the vertical total electron content (VTEC) at the Arbaminch station during the days surrounding the partial solar eclipse of January 26, 2009.*

The graph illustrates the VTEC variations at Arbaminch station, Ethiopia, during the partial solar eclipse on January 26, 2009 (04: 57- 09: 55 UT), which reached a maximum obscuration of 45- 55%. On the reference day of 25 January 2009 (before the eclipse), TEC varied from 7 TECU to 19 TECU during the eclipse period (05: 00–10: 00 UT). On 27 January 2009 (after the eclipse), TEC ranged from 7 TECU to 18 TECU. However, on the eclipse day of 26 January 2009, TEC varied from 7 TECU to 17 TECU, which was the minimum compared to the selected reference days.

The graph reveals how the dip in the green line (January 26) during the red-shaded eclipse period reflects a significant reduction in ionospheric electron density due to diminished solar EUV radiation. This contrasts with the steady daytime rise on January 25 (blue line) and the recovery on January 27 (black line), highlighting the eclipse's localized atmospheric effects and the critical role of solar radiation in ionospheric dynamics.

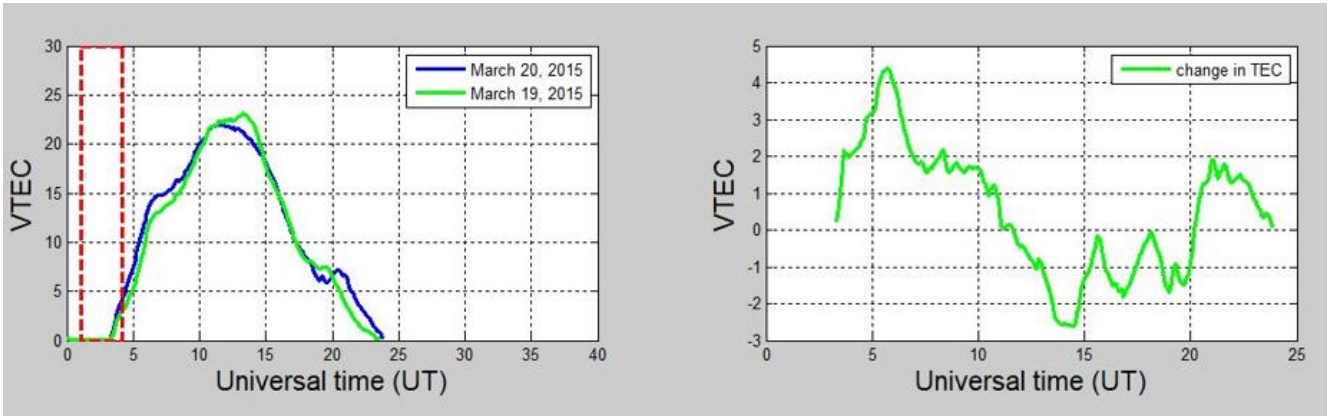

Figure 5. *Shows a comparison of vertical total electron content (VTEC) variations and the differences in TEC before and during the solar eclipse on March 20, 2015, at Robe station.*

The left panel shows VTEC variations at Robe station, Ethiopia, comparing March 20, 2015 (blue curve; partial solar eclipse day) with March 19, 2015 (green curve, reference day). The eclipse 01: 12-03: 05 UT, peaking at ~02: 24 UT) significantly affects VTEC.

On the reference day of 19 march 2015 (before the eclipse), TEC varied from 0 TECU to 05 TECU during the eclipse period (01: 03 to 03: 05 UT). However, on the eclipse day On 20 March 2015, TEC varied from 0 TECU to 04 TECU.

During the red-dotted interval (corresponding to the eclipse), the blue curve exhibits a delayed and weaker increase compared to the green reference line.

The right panel illustrates VTEC changes at Robe station, Ethiopia, during the partial solar eclipse on March 20, 2015. The green curve highlights deviations from the March 19, 2015, reference baseline. The data reveal significant fluctuations: a sharp initial increase followed by a pronounced dip, reflecting the eclipse's impact on ionospheric electron density. The eclipse (01: 12–03: 05 UT; maximum obscuration 02: 24 UT) likely drives the positive spike via partial solar obscuration response, followed by a negative excursion due to reduced solar radiation and suppressed electron production a common pattern in low-latitude regions [13]. The right panel shows the change in TEC on March 20, 2015, relative to the reference day, and it highlights the eclipse effect more clearly. During the eclipse interval (01: 12 - 03: 05 UT), there is a positive deviation in TEC, followed by a sharp fluctuation as the obscuration progresses toward maximum and then declines. The peak change occurs close to the maximum obscuration time (around 02: 24 UT), showing that the eclipse significantly altered the normal ionization pattern in the ionosphere. After the eclipse ends, the curve continues to show irregular variations, which may reflect the combined influence of both the eclipse recovery process and the background moderate geomagnetic disturbance present on that day. Overall, this graph demonstrates that the eclipse caused distinct and measurable fluctuations in ionospheric TEC compared to a quiet reference day.

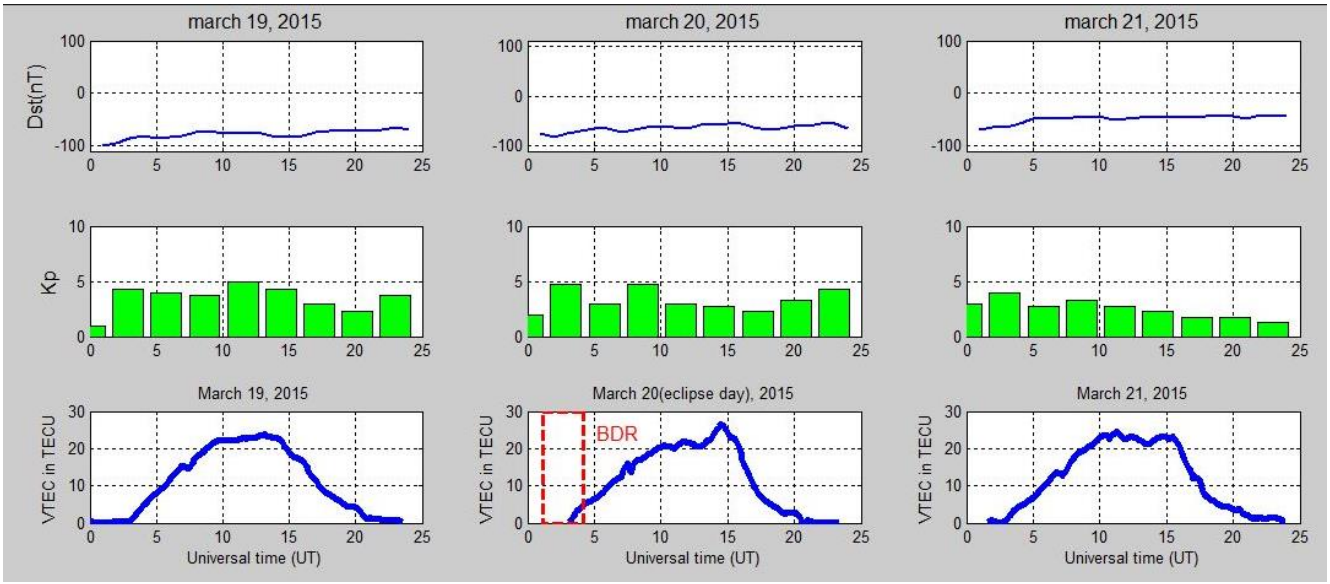

Figure 6. *Shows the diurnal variations of the vertical total electron content (VTEC) and geomagnetic disturbance with DST and KP indices at Bahir Dar station during the days surrounding the partial solar eclipse of March 20, 2015.*

The graphs illustrate geomagnetic and ionospheric conditions over three days March 19, 20, and 21, 2015 with a notable partial solar eclipse occurring in Ethiopia on March 20, 2015, starting at 01: 11: 58 UTC, peaking at 02: 24: 12 UTC, and ending at 03: 04: 44 UTC.

The comparison of these three consecutive days clearly demonstrates the effect of the partial solar eclipse on March 20, 2015, over BDR. The Dst index remains nearly the same across the three days, maintaining values around - 80 nT, which indicates similar geomagnetic storm conditions and rules out geomagnetic activity as the main cause of VTEC [38, 40].

The Kp index also shows only moderate activity around 5, further confirming that geomagnetic conditions were stable throughout the period. On the non-eclipse days (March 19 and 21), the VTEC curve follows a normal diurnal pattern, rising rapidly after sunrise due to increasing solar radiation, peaking around local noon, and then declining gradually toward evening.

However, on the eclipse day (March 20), during the time interval marked by the red dotted box, the rate of increase of TEC is significantly reduced compared to the other two days. This suppression occurs because the partial solar obscuration reduces the amount of extreme ultraviolet (EUV) radiation reaching the ionosphere, thus lowering the rate of ionization in the F-region [41-43]. Even after the eclipse interval, the TEC continues to recover slowly, indicating a delayed response of the ionosphere as it takes time for normal ionization levels to be restored [35, 44-46]. The maximum TEC value on the eclipse day is slightly smaller and occurs later than on

March 19 and 21, reflecting the reduced production of electrons due to the temporary loss of solar radiation. The partial solar eclipse clearly caused a temporary depletion and slower recovery of TEC, showing its noticeable but limited effect on the ionosphere [47-49].

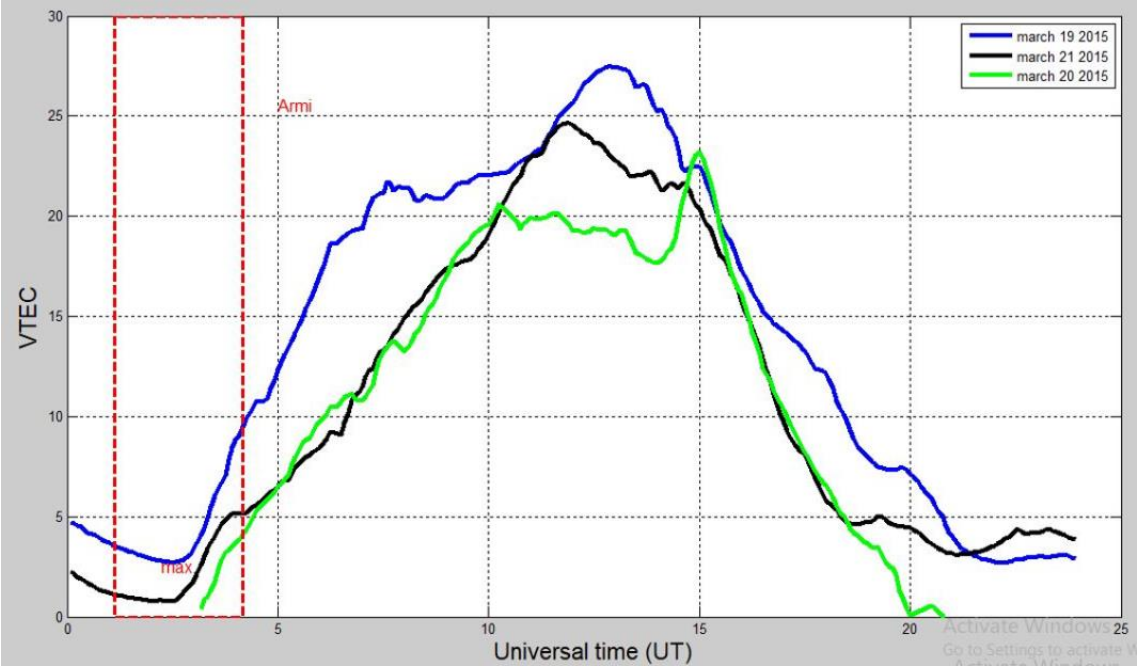

Figure 7. *Shows the diurnal variations of the VTEC at Arba Minch station during the days surrounding the partial solar eclipse of March 20, 2015.*

The graph depicts the temporal variation in VTEC over the Arba Minch station in Ethiopia during the partial solar eclipse on March 20, 2015. It is overlaid with data from the preceding day (March 19) and following day (March 21) for comparative context. The eclipse event commenced around 01: 12 UT, reached maximum obscuration at approximately 02: 24 UT, and concluded near 03: 05 UT, as indicated by the red vertical dotted lines marking the start, maximum, and end phases. Between the eclipse time interval indicated by the red dotted lines (from 01: 12 UT to 03: 05 UT), the green curve representing March 20, 2015, shows a clear depression in VTEC compared to the control days (March 19 and 21). At the beginning of the eclipse (01: 12 UT), the VTEC starts to rise more slowly than on the non-eclipse days, and around the maximum eclipse 02: 24 UT, the VTEC reaches its lowest relative level, indicating the strongest reduction in ionization due to maximum solar obscuration [50]. This reduced ionization occurs because the temporary blockage of solar radiation by the Moon limits the production of free electrons in the ionosphere [20, 51, 52]. After the maximum phase and toward the end of the eclipse 03: 05 UT, the VTEC begins to recover but still lags behind the reference days, showing a delayed response of the ionosphere to the returning solar radiation. Overall, the graph during this interval clearly demonstrates the suppressive effect of the solar eclipse on electron density in the ionosphere.

The spatial comparison of VTEC during the solar eclipse on January 26, 2009, at the Bahir Dar, Arbaminch, and Robe stations revealed no distinct differences in VTEC variation. This is because all the stations are located in Ethiopia, with no great geographical differences between them. Total electron content is strongly dependent on solar radiation and photoionization [53-55].

In addition to the partial solar eclipse of January 26, 2009, the event of March 20, 2015, at the Bahir Dar, Arbaminch, and Robe stations also showed no distinct differences in VTEC variation. This is because all the stations are located in Ethiopia, with no significant differences in latitude and longitude between them. However, we observed greater TEC variations during solar maximum compared to solar minimum conditions. Specifically, the maximum TEC was 18 TECU during the January 26, 2009 eclipse and 28 TECU during the March 20, 2015 eclipse. This implies that TEC values are strongly influenced by the amount of solar radiation in the atmosphere when regions have no substantial differences in geographical location [56, 57].

4. Conclusion

We have shown solar eclipse-induced variations in Total Electron Content (TEC) over Ethiopia, focusing on the partial

solar eclipses of March 20, 2015, and January 26, 2009. During the eclipse interval, the data clearly demonstrate the suppressive effect of the solar eclipse on electron density in the ionosphere. The variation of vertical Total Electron Content (VTEC) over Bahir Dar station during the days surrounding the partial solar eclipse of January 26, 2009, is noteworthy. On the reference days, January 25 and 27, the VTEC values show a typical diurnal pattern gradually increasing after sunrise, peaking during midday, and then decreasing toward night time. However, on January 26, the eclipse day, a noticeable depression in VTEC is observed during the eclipse interval, which began at 04: 57 UT, reached its maximum obscuration at 07: 59: 44 UT, and ended around 09: 55 UT. This reduction corresponds to the temporary decrease in solar radiation reaching the Earth's ionosphere, limiting ionization and thus lowering the electron density compared to non-eclipse days. After the eclipse ended, the VTEC trend gradually recovered and followed a relatively normal pattern.

On January 26, the eclipse day, a significant depression in VTEC was observed during the eclipse interval, which began at 04: 57 UT, reached its maximum obscuration (55–65%) at 07: 59: 44 UT, and concluded around 09: 55 UT. This reduction correlates with the temporary decrease in solar radiation reaching the Earth's ionosphere, limiting ionization and consequently lowering electron density compared to non-eclipse days. Following the eclipse, the VTEC trend gradually recovered, reverting to typical diurnal patterns. The VTEC variations observed over the Bahir Dar station during January 25–27, 2009, clearly demonstrate the ionospheric response to the partial solar eclipse on January 26, 2009. On non-eclipse days (January 25 and 27, 2009), TEC followed a standard diurnal pattern rising after sunrise, peaking around midday, and decreasing toward night.

The comparison of TEC variation on consecutive days reveals that, on the reference day of 19 March 2015 (before the eclipse), the maximum VTEC was approximately 26 TECU. In contrast, on 20 March 2015 (the eclipse day), the maximum VTEC was approximately 24 TECU. This clearly demonstrates the effect of the partial solar eclipse on March 20, 2015, over BDR. The VTEC variations observed at the Robe station on 20 March 2015 show an approximate 20% reduction, corresponding to the temporary decrease in solar radiation reaching Earth's ionosphere.

Abbreviations

UT	Universal Time
GPS	Global Positioning System
VTEC	Vertical Total Electron Content
EUV	Extreme Ultraviolet
Kp	Planetary K-index
Dst	Disturbance Storm Time index
ARMI	Arbaminch
BDR	Bahir Dar

Acknowledgments

We would like to convey our sincere appreciation to UNAVCO Data Center for their free access to GPS and geomagnetic data.

Author Contributions

Debrie Ayalew: Writing – original draft, Methodology, Investigation

Shambel Gizachew: Writing – review & editing, Visualization

Melkamu Habtamu: Formal Analysis, Data curation

Data Availability Statement

The data that has been used is confidential and it will be made available on request.

Conflicts of Interest

The authors declare no conflicts of interest relevant to this study.

References

[1] Okoh, D., et al., Total Electron Content Variations Over Abuja During the Annular Solar Eclipse of September 1, 2016.

[2] Cooper, C., et al., Measurement of ionospheric total electron content using single-frequency geostationary satellite observations. Radio Science, 2019. 54(1): p. 10-19.

[3] Guo, L., et al. Ionospheric response to the total solar eclipse of 22 july 2009 as deduced from VLBI and GPS Data. in Proceedings of the Sixth General Meeting of the International VLBI Service for Geodesy and Astrometry. 2010.

[4] Correia, E., et al., Characterization of the ionosphere response to the X1. 3 solar event occurred on 30 March 2022. Advances in Space Research, 2025.

[5] Wang, S., et al., Analysis of the consecutive X-ray flares effects on the lower ionosphere. Space Weather, 2025. 23(8): p. e2025SW004471.

[6] Jenan, R., T. L. Dammalage, and S. K. Panda, Ionospheric total electron content response to September-2017 geomagnetic storm and December-2019 annular solar eclipse over Sri Lankan region. Acta Astronautica, 2021. 180: p. 575-587.

[7] Prölss, G., Physics of the Earth's space environment: an introduction. 2012: Springer Science & Business Media.

[8] Tariku, Y. A., Patterns of GPS-TEC variation over low-latitude regions (African sector) during the deep solar minimum (2008 to 2009) and solar maximum (2012 to 2013) phases. Earth, Planets and Space, 2015. 67(1): p. 35.

[9] Davies, K., Ionospheric radio propagation. Vol. 80. 1965: US Department of Commerce, National Bureau of Standards.

[10] Dessler, A., J. T. Houghton, and M. J. Rycroft, Cambridge atmospheric and space science series. (No Title), 2001.

[11] Kelley, M. C., The Earth's ionosphere: Plasma physics and electrodynamics. Vol. 96. 2009: Academic press.

[12] Huang, Z. and R. Roussel-Dupré, Total electron content (TEC) variability at Los Alamos, New Mexico: A comparative study: FORTE-derived TEC analysis. Radio science, 2005. 40(06): p. 1-23.

[13] Uga, C. I., et al., Variation in total electron content over Ethiopia during the solar eclipse events. Radio Science, 2024. 59(4): p. e2023RS007830.

[14] Aa, E., et al., 2-D total electron content and 3-D ionospheric electron density variations during the 14 October 2023 annular solar eclipse. Journal of Geophysical Research: Space Physics, 2024. 129(3): p. e2024JA032447.

[15] Jose, L., et al., Response of the equatorial ionosphere to the annular solar eclipse of 15 January 2010. Journal of Geophysical Research: Space Physics, 2020. 125(8): p. e2019JA027348.

[16] Athwart, D. O., B. Ndinya, and P. Baki, Effects of 15th January 2010 Annular Solar Eclipse on Traveling Ionospheric Disturbances and Equatorial Plasma Bubbles over Low Latitude Regions of East Africa. Advances in Astronomy, 2022. 2022(1): p. 5263997.

[17] Adeniyi, J., et al., Signature of the 29 March 2006 eclipse on the ionosphere over an equatorial station. Journal of Geophysical Research: Space Physics, 2007. 112(A6).

[18] Da Silva, A., et al., A multi-instrumental and modelling analysis of the ionospheric responses to the solar eclipse of December 14, 2020, over the Brazilian region.

[19] Hoque, M. M., et al., Ionospheric response over Europe during the solar eclipse of March 20, 2015. Journal of Space Weather and Space Climate, 2016. 6: p. A36.

[20] Sanyal, A., et al., Investigation of the Ionospheric Effects of the Solar Eclipse of April 8, 2024 Using Multi-Instrument Measurements. Atmosphere, 2025. 16(2): p. 161.

[21] Silwal, A., et al., Global positioning system observations of ionospheric total electron content variations during the 15th January 2010 and 21st June 2020 solar eclipse. Radio Science, 2021. 56(5): p. e2020RS007215.

[22] Tilahun, A. M., et al., Equatorial ionospheric VTEC perturbations during the 21 June 2020 solar eclipse. Earth and Space Science, 2025. 12(12): p. e2025EA004366.

[23] Kumar, S., et al., Changes in the D region associated with three recent solar eclipses in the South Pacific region. Journal of Geophysical Research: Space Physics, 2016. 121(6): p. 5930-5943.

[24] Ciraolo, L., et al., Calibration errors on experimental slant total electron content (TEC) determined with GPS. Journal of geodesy, 2007. 81(2): p. 111-120.

[25] Mayer, C., et al., Extreme ionospheric conditions over Europe observed during the last solar cycle. 2008.

[26] Jain, A., et al., TEC response during severe geomagnetic storms near the crest of equatorial ionization anomaly. Indian J. Radio Space Phys, 2010. 39: p. 11-24.

[27] Ismail, M., Total Electron Content (TEC) and Estimation of Positioning Error Using Malaysia Data.

[28] Yasyukevich, Y. V., A. Mylnikova, and A. Polyakova, Estimating the total electron content absolute value from the GPS/GLONASS data. Results in Physics, 2015. 5: p. 32-33.

[29] Kersley, L., et al., Total electron content-A key parameterin propagation: measurement and usein ionospheric imaging. Annals of Geophysics, 2004. 47(2-3 Sup.).

[30] Wanninger, L., Effects of the equatorial ionosphere on. GPS world, 1993.

[31] Ya'acob, N., M. Abdullah, and M. Ismail, Determination of GPS total electron content using single layer model (SLM) ionospheric mapping function. International Journal of Computer Science and Network Security, 2008. 8(9): p. 154-160.

[32] Zhao, B., et al. Characteristics of the ionospheric total electron content of the equatorial ionization anomaly in the Asian-Australian region during 1996–2004. in Annales Geophysicae. 2009. Copernicus Publications Göttingen, Germany.

[33] Lay, E. H., et al., New lightning-derived vertical total electron content data provide unique global ionospheric measurements. Space Weather, 2022. 20(5): p. e2022SW003067.

[34] Fedrizzi, M., et al., Mapping the low-latitude ionosphere with GPS. GPS WORLD, 2002. 13(2): p. 41-47.

[35] Ogwala, A., et al. Diurnal, seasonal and solar cycle variation in total electron content and comparison with IRI-2016 model at Birnin Kebbi. in Annales Geophysicae. 2019. Copernicus Publications Göttingen, Germany.

[36] Chen, C., et al., Ionospheric responses on the 21 August 2017 solar eclipse by using three-dimensional GNSS tomography. Earth, Planets and Space, 2022. 74(1): p. 173.

[37] Gómez, D. D., Ionospheric response to the December 14, 2020 total solar eclipse in South America. Journal of Geophysical Research: Space Physics, 2021. 126(7): p. e2021JA029537.

[38] Paul, A., et al. Response of the equatorial ionosphere to the total solar eclipse of 22 July 2009 and annular eclipse of 15 January 2010 as observed from a network of stations situated in the Indian longitude sector. in Annales geophysicae. 2011. Copernicus Publications Göttingen, Germany.

[39] Abraha, G., A. Msganaw, and T. Kassa, Solar activity and geomagnetic storm effects on gps ionospheric tec over Ethiopia. Momona Ethiopian Journal of Science (MEJS), 2019. 11(2): p. 276-300.

[40] Mendillo, M., Storms in the ionosphere: Patterns and processes for total electron content. Reviews of Geophysics, 2006. 44(4).

[41] Srigutomo, W., et al., Decrease of total electron content during the 9 March 2016 total solar eclipse observed at low latitude stations, Indonesia. Annales Geophysicae Discussions, 2019. 2019: p. 1-12.

[42] Chakraborty, S., et al., Modeling of the lower ionospheric response and VLF signal modulation during a total solar eclipse using ionospheric chemistry and LWPC. Astrophysics and Space Science, 2016. 361(2): p. 72.

[43] Vaishnav, R., et al., Ionospheric response to solar EUV radiation variations using GOLD observations and the CTIPe model. Journal of Geophysical Research: Space Physics, 2024. 129(1): p. e2022JA030887.

[44] Resende, L. C., et al. A multi-instrumental and modeling analysis of the ionospheric responses to the solar eclipse on 14 December 2020 over the Brazilian region. in Annales Geophysicae. 2022. Copernicus Publications Göttingen, Germany.

[45] Alizadeh, M. M., et al., Remote sensing ionospheric variations due to total solar eclipse, using GNSS observations. Geodesy and Geodynamics, 2020. 11(3): p. 202-210.

[46] Liu, J., et al., Ionospheric response to the 21 May 2012 annular solar eclipse over Taiwan. Journal of Geophysical Research: Space Physics, 2019. 124(5): p. 3623-3636.

[47] Lei, J., et al., Long-lasting response of the global thermosphere and ionosphere to the 21 August 2017 solar eclipse. Journal of Geophysical Research: Space Physics, 2018. 123(5): p. 4309-4316.

[48] Abadi, P., et al., Observations of Ionospheric Conditions Over Pontianak During The Partial Solar Eclipse. Indonesian Journal of Aerospace, 2024. 22(2): p. 85-94.

[49] Paulino, I., et al., Ionospheric responses to the 14 October 2023 annular solar eclipse over Brazil: A case study of fixed-frequency isoline variations. EGUsphere, 2026. 2026: p. 1-16.

[50] Harjosuwito, J., et al. Ionosonde and GPS total electron content observations during the 26 December 2019 annular solar eclipse over Indonesia. in Annales Geophysicae. 2023. Copernicus Publications Göttingen, Germany.

[51] Singh, R., et al., D-region ionosphere response to the total solar eclipse of 22 July 2009 deduced from ELF-VLF tweek observations in the Indian sector. Journal of Geophysical Research: Space Physics, 2011. 116(A10).

[52] Eshkuvatov, H., et al., Variations in Ionospheric Total Electron Content and Scintillation at GPS stations in Uzbekistan and China during the Annular Solar Eclipse on June 21, 2020. Physics of the Dark Universe, 2025. 48: p. 101892.

[53] Afraimovich, E., E. Kosogorov, and O. Lesyuta, Effects of the August 11, 1999 total solar eclipse as deduced from total electron content measurements at the GPS network. Journal of atmospheric and solar-terrestrial physics, 2002. 64(18): p. 1933-1941.

[54] Hassan, Z., et al., Investigating Ionospheric TEC Variations in Solar and Geomagnetic Influences Across Solar Activity Phases. Advances in Space Research, 2026.

[55] Le, H., et al., Anomaly distribution of ionospheric total electron content responses to some solar flares. Earth and Planetary Physics, 2019. 3(6): p. 481-488.

[56] Homam, M., The correlation between total electron content variations and solar activity. 2015.

[57] Hargreaves, J. K., The solar-terrestrial environment: an introduction to geospace-the science of the terrestrial upper atmosphere, ionosphere, and magnetosphere. 1992: Cambridge university press.